

# Centroid Transformers: Learning to Abstract with Attention

Lemeng Wu \*

UT Austin

lmwu@cs.utexas.edu

Xingchao Liu \*

UT Austin

xcliu@utexas.edu

Qiang Liu

UT Austin

lqiang@cs.utexas.edu

## Abstract

Self-attention, as the key block of transformers, is a powerful mechanism for extracting features from the inputs. In essence, what self-attention does is to infer the *pairwise relations* between the elements of the inputs, and modify the inputs by propagating information between the input pairs. As a result, it maps  $N$  inputs to  $N$  outputs and casts a quadratic  $O(N^2)$  memory and time complexity. We propose *centroid attention*, a generalization of self-attention that maps  $N$  inputs to  $M$  outputs ( $M \leq N$ ), such that the key information in the inputs is summarized in the smaller number of outputs (called centroids). We design centroid attention by amortizing the gradient descent update rule of a clustering objective function on the inputs, which reveals a underlying connection between attention and clustering. By compressing the inputs to the centroids, we extract the key information useful for prediction and also reduce the computation of the attention module and the subsequent layers. We apply our method to various applications, including abstractive text summarization, 3D vision, and image processing. Empirical results demonstrate the effectiveness of our method over the standard transformers.

## 1 INTRODUCTION

Recently, transformer (Vaswani et al., 2017) has emerged to be one of the most important neural architectures and has achieved remarkable successes on various tasks such as language modeling (Irie et al., 2019; Jiao et al., 2020), machine translation (Vaswani et al., 2017; Zhang et al., 2018; Wang et al., 2019a), computer vision (Carion et al., 2020; Dosovitskiy et al., 2020), and many others.

What makes transformers unique is the extensive usage of the self-attention mechanism (Vaswani et al., 2017). A self-attention block is placed in each stage of the transformer to gather information *globally* from the input sequence. A self-attention module takes in  $N$  inputs, and returns  $N$  outputs of the same size. For each element in the input, it assigns an attention weight to every other element in the input to find out who it should pay more attention to, and perform a weighted sum to aggregate the information from the relevant inputs.

Intuitively, the self-attention modules can be viewed as conducting *interactive reasoning*, inferring the pairwise interacting relations between the elements of inputs and propagating information between pairs of elements. Naturally, a key drawback of the pairwise interaction is that it casts an  $O(N^2)$  memory and time complexity, where  $N$  is the number of input elements, making it a major computational bottleneck in transformers. This necessitates an emerging line of research on approximating self-attention modules to gain higher computational efficiency (Kitaev et al., 2019; Katharopoulos et al., 2020; Wang et al., 2020).

In this work, we develop a variant of attention module for conducting *summative reasoning* rather than *interactive reasoning*. Our goal is to take  $N$  input elements and return a smaller number  $M$  of outputs ( $M \leq N$ ), such that the key information in the  $N$  inputs are summarized in the  $M$  outputs. If  $N = M$ , our new module reduces to standard self-attention (except an extra skip connection link). However, by setting  $M < N$ , we creates an information bottleneck and enforce the network to filter out the useless information (i.e., dimension reduction), and also improve the computational cost from  $O(N^2)$  to  $O(NM)$ . In addition, once the number of inputs is reduced, the complexity of the subsequent modules/layers is also reduced accordingly (e.g., applying self-attention on the output will yield a  $O(M^2)$  complexity).

Intuitively, we hope that the  $M$  output elements are representative of the  $N$  inputs. This can be viewed as a clustering process in which we find  $M$  “centroids” for the inputs. Our new module, which we call *centroid attention layer*, is obtained by “*amortizing*” the *gradient descent update rule on a clustering objective function*. It exploits a novel connection between self-attention and clustering algorithms: we write down a clustering objective function on the input data under a trainable similarity metric, and derive its gradient descent update rule; we then observe that the gradient descent update yields a generalization of self-attention layer and use it to motivate the design of our new module.

Using our new modules, we build *centroid transformers*, in which we insert our centroid attention modules between typical self-attention modules. We apply centroid transformers on several challenging scenarios, ranging from natural language processing to computer vision. On ab-

---

\*Equal contribution

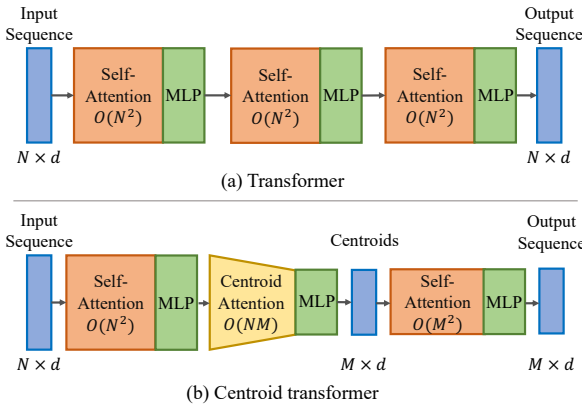


Figure 1: The vanilla transformer (a) which maps  $N$  inputs to  $N$  outputs; and our centroid transformer (b) which summarizes  $N$  inputs into  $M$  “centroid” outputs ( $M \leq N$ ) to save computational cost and filter out useless information simultaneously.

stractive text summarization, centroid transformer beats the vanilla transformer with about only 50% computational cost. On 3D point cloud classification and image classification tasks, centroid transformer achieves substantially higher accuracy as well as computational efficiency compared with the state-of-the-art transformer networks. We also use centroid attention to replace the dynamic routing module in the 3D Capsule Network (Zhao et al., 2019) for point cloud reconstruction, which we find yields lower construction error, reduced storage consumption, and more semantically meaningful latent representation.

## 2 CENTROID TRANSFORMER

We first introduce the standard self-attention mechanism used in vanilla transformers in Section 2.1, and then derive the centroid attention mechanism by drawing inspiration from the gradient descent update of a clustering objective function and discuss the related centroid transformer in Section 2.2.

### 2.1 SELF-ATTENTION MECHANISM

Let  $\{\mathbf{x}_i\}_{i=1}^N \in \mathbb{R}^{N \times d}$  be a set of input vectors, where we may view each vector  $\mathbf{x}_i$  as a data point or “particle”. Each  $\mathbf{x}_i$  can be a word embedding vector in natural language processing, an image patch in computer vision, or a point in 3D point cloud. A self-attention module can be viewed as updating  $\{\mathbf{x}_i\}$  in parallel via

$$\mathbf{x}'_i \leftarrow \mathbf{x}_i + \epsilon \sum_{j=1}^N \sum_{\ell=1}^L \text{sim}_\ell(\mathbf{x}_i, \mathbf{x}_j) \times v_\ell(\mathbf{x}_j), \quad \forall i \in [N] \quad (1)$$

Here, each  $\text{sim}_\ell(\cdot, \cdot)$  is a similarity function and  $v_\ell(\mathbf{x}_i) \in \mathbb{R}^d$  is a value function; each  $\ell$  is considered to be a head in the attention and process a specific aspect of the inputs;  $\epsilon$  is a positive constant.

Intuitively, the self-attention module evaluates the similarity (or attention score) between pairs of input vectors, and updates each vector with the sum of the inputs weighted by the similarity scores. In practice, the similarity function is often defined as

$$\text{sim}_\ell(\mathbf{x}_i, \mathbf{x}_j) = \frac{\exp(Q_\ell^\top(\mathbf{x}_i)K_\ell(\mathbf{x}_j))}{\sum_{k=1}^N \exp(Q_\ell^\top(\mathbf{x}_i)K_\ell(\mathbf{x}_k))}, \quad (2)$$

where  $Q_\ell(\mathbf{x})$  and  $K_\ell(\mathbf{x})$  are the “query” and “key” functions of the  $\ell$ -th head. Eq. (1) and (2) illustrate how the features are processed by one head. A complete transformer encoder with  $T$  layers is the composition of self-attention layers and multi-layer perceptrons (MLPs); see Figure 1. Obviously, the time and memory complexities of self-attention are quadratic on  $N$ , i.e.,  $O(N^2)$ , which form the key computational bottleneck when applying self-attention on long sequences and large batches of data.

### 2.2 CENTROID ATTENTION

Self-attention updates the inputs  $\{\mathbf{x}_i\}$  based on their interacting relations, obtaining an output of the same size. In this work, we propose a mechanism that maps the  $N$  inputs  $\{\mathbf{x}_i\}_{i=1}^N$  to  $M$  output vectors  $\{\mathbf{u}_i\}_{i=1}^M$ ,  $M \leq N$ , such that each  $\mathbf{u}_j \in \mathbb{R}^d$  can be viewed as a centroid of the inputs  $\{\mathbf{x}_i\}_{i=1}^N$ . Namely, we hope the module to be able to effectively perform a clustering-like operation on the inputs, where  $\{\mathbf{u}_i\}_{i=1}^M$  is a compression of  $\{\mathbf{x}_i\}_{i=1}^M$  while inheriting the key information.

Let  $\{\phi_\ell(\mathbf{x}_i, \mathbf{u}_j) : \forall \ell \in [L]\}$  be a set of measures of similarity between centroid  $\mathbf{u}_j$  and input  $\mathbf{x}_i$ . Ideally, we may want to construct the centroids by optimizing the following general “soft K-means” objective function for clustering,

$$\{\mathbf{u}_j^*\} = \arg \max_{\{\mathbf{u}_j\}} \sum_{\ell=1}^L \sum_{i=1}^N \frac{1}{\alpha} \log \left( \sum_{j=1}^M \exp(\alpha \phi_\ell(\mathbf{x}_i, \mathbf{u}_j)) \right). \quad (3)$$

Here,  $\alpha > 0$  is a positive coefficient. If  $\alpha \rightarrow +\infty$  and  $L = 1$ , then the objective reduces to  $\sum_i \max_j \phi_1(\mathbf{x}_i, \mathbf{u}_j)$ , which coincides with the typical k-means objective function when  $-\phi_1(\cdot, \cdot)$  is a distance measure. In general, the objective (3) obtains centroids to represent the inputs based on multiple similarity functions  $\{\phi_\ell\}$ .

By solving the optimization with gradient descent, we can unroll (3) into an iterative update of form:

$$\text{Initialization: } \{\mathbf{u}_j^0\}_{j=1}^M = I(\{\mathbf{x}_i\}_{i=1}^N)$$

For  $t = 1, 2, \dots, T$ ,

$$\mathbf{u}_j^{t+1} \leftarrow \mathbf{u}_j^t + \epsilon \sum_{\ell=1}^L \sum_{i=1}^N \text{sim}_\ell(\mathbf{x}_i, \mathbf{u}_j^t) V_\ell(\mathbf{x}_i, \mathbf{u}_j^t), \quad (4)$$

where  $I(\cdot)$  denotes a mechanism for initializing the centroids and each of the following  $T$  steps conducts gradient

descent of (3), with

$$\text{sim}_\ell(\mathbf{x}_i, \mathbf{u}_j) = \frac{\exp(\alpha\phi_\ell(\mathbf{x}_i, \mathbf{u}_j))}{\sum_{k=1}^M \exp(\alpha\phi_\ell(\mathbf{x}_i, \mathbf{u}_k))},$$

$$V_\ell(\mathbf{x}_i, \mathbf{u}_j) = \nabla_{\mathbf{u}_j} \phi_\ell(\mathbf{x}_i, \mathbf{u}_j).$$

Clearly, the gradient update above can be interpreted as a multi-head attention mechanism, with  $\text{sim}_\ell(\cdot, \cdot)$  and  $V_\ell(\cdot, \cdot)$  being the similarity function and the value function of the  $\ell$ -th head. The initialization  $I(\cdot)$  together with the  $T$  steps of attention like updates in (4) above form a *centroid attention module*. See Figure 2 for an illustration.

In practice, we find it works well to set  $\epsilon = 1/T$  by default. Moreover, in settings when computational efficiency is important, we set  $T = 1$  for a good performance-efficiency trade off. The initialization step can vary in different tasks: we can, for example, draw  $\{\mathbf{u}_j^0\}_{j=1}^M$  from  $\{\mathbf{x}_i\}_{i=1}^N$  by random sampling without replacement or farthest point sampling; we can also directly define  $I(\cdot)$  to be a trainable fully connected or convolution layer. See more discussion in the experiment section.

Although both  $\text{sim}_\ell(\cdot, \cdot)$  and  $V_\ell(\cdot, \cdot)$  are determined by  $\phi_\ell$  following the derivation above. In practice, we can define them separately in more flexible forms based on practical needs. For example, we may define  $\text{sim}_\ell(\cdot, \cdot)$  by setting  $\phi(\mathbf{x}_i, \mathbf{u}_j) = Q_\ell^\top(\mathbf{u}_j)K(\mathbf{x}_i)$  as typical self-attention, while setting  $V_\ell(\mathbf{x}_i, \mathbf{u}_j)$  with a separate trainable value function.

Our module includes self-attention as a special case when we *i*) set  $M = N$ , *ii*) initialize  $\{\mathbf{u}_i\}$  to be the same as  $\mathbf{x}_i$ , and *iii*) iterate for one step ( $T = 1$ ). Therefore, our derivation also reveals a close connection between gradient-based clustering and self attention. Note that Ramsauer et al. (2020) discusses a connection between Hopfield update rule and self-attention, which is related but different from our perspective.

**KNN Approximation** The computational cost of the attention is  $O(NM)$ , which can still be expensive if  $N$  and  $M$  are large. To further save the computational cost, we apply a K-nearest neighbor (KNN) approximation to (4), yielding

$$\mathbf{u}_j^{t+1} \leftarrow \mathbf{u}_j^t + \epsilon \sum_{\ell=1}^L \sum_{i \in \mathcal{N}_{j,k}^\ell} \text{sim}_\ell(\mathbf{x}_i, \mathbf{u}_j^t) V_\ell(\mathbf{x}_i, \mathbf{u}_j^t),$$

where  $\mathcal{N}_{j,k}^\ell$  denotes the K-nearest neighbor of  $\mathbf{u}_j$  inside  $\{\mathbf{x}_i\}_{i=1}^N$ , that is,  $\mathcal{N}_{j,k}^\ell = \{i_{(1)}, \dots, i_{(k)}\}$ , where  $\{i_{(1)}, \dots, i_{(n)}\}$  is the ascending reordering of  $\{1, \dots, n\}$  according to some distance metric  $d(\mathbf{x}_i, \mathbf{u}_j)$ . In practice, we define the distance by  $d(\mathbf{x}_i, \mathbf{u}_j) = \|\mathbf{x}_i - \mathbf{u}_j\|_2$ .

As shown in our experiments, the KNN approximation is particularly useful for the point cloud classification task, in which the length of the inputs elements is  $N = 1024$ , which is beyond the capacity of our GPU memory even for a single data point (i.e., a batch size of 1).

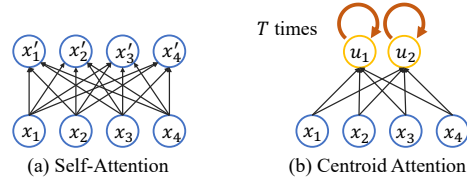


Figure 2: (a) The self-attention module, which modifies the input sequence  $\{\mathbf{x}_i\}$  into  $\{\mathbf{x}'_i\}$  by updating them with pairwise interactions (see Eq (1)). (b) The centroid attention module, which transforms the input sequence  $\{\mathbf{x}_i\}$  into a set of centroids  $\{\mathbf{u}_i\}$  by first initializing the centroids and then updating them by interacting with the elements in the inputs (see Eq (4)).

**Centroid Transformer** As shown in Fig. 1, we construct a centroid transformer architecture by alternating between typical self-attention blocks and centroid attention blocks. This allows us to gradually abstract the input sequence to increasingly short representations, which filters out useless information and simultaneously saves the computation cost. As vanilla transformer, we insert fully connected MLP layers with residual links between the attention modules.

### 3 EXPERIMENTS

We apply our centroid attention block on different kind of tasks with transformer or capsule structures to show our powerful abstract ability as well as the computational efficiency. We show that our centroid transformer structure has a strong performance in various of tasks including text summarization, point cloud classification, point cloud reconstruction and image classification. On all the tasks, we outperform baseline transformer with lower computational and storage cost.

#### 3.1 ABSTRACTIVE TEXT SUMMARIZATION

We test centroid transformer on abstractive text summarization, a classic task in natural language processing. The task is to provide a short summary text (in several words) for a paragraph or a long sentence.

**Data** We use the annotated Gigaword corpus (Rush et al., 2015) as our benchmark to compare different methods. The dataset is pre-processed with the tools provided by the authors. The corpus contains about 3.8 millions of training examples. The script also has 400,000 extra examples for validation and test. We randomly sample 2,000 examples for validation and test respectively, as in Nallapati et al. (2016). All the models are validated and tested with the same validation and test set. The performance of the generated summaries is measured by Recall-Oriented Understudy for Gisting Evaluation (ROUGE) (Lin, 2004). ROUGE-1/ROUGE-2/ROUGE-L

Models	MACs(M)	MBS/GPU	ROUGE-1	ROUGE-2	ROUGE-L
Transformer	523.2	192	32.987	15.286	30.771
Ours-Random	<b>262.9</b>	<b>230</b>	30.310	12.752	27.823
<b>Ours-MP</b>	<b>262.9</b>	<b>230</b>	<b>34.651</b>	<b>16.468</b>	<b>32.415</b>

Table 1: Results on Gigaword text summarization task (MBS=Maximal Batch Size, MP = Mean-Pooling). The MACs (Multiply-add ACcumulation) is only computed for the encoder, assuming the length of sequence is 45 (the maximal length of sequence in the dataset). Though centroid transformer with random initialization (Ours-Random) performs worse than the baseline, centroid transformer with mean-pooling being the initialization method (Ours-MP) yields the best ROUGE score (See (Lin, 2004) for its definition) with 50% computational cost compared to the original transformer.

evaluates the quality of unigrams/bigrams/whole sentence in the generated summary.

**Model Configuration** We construct our centroid transformer by replacing the second self-attention module in the baseline transformer encoder with our centroid attention module.

$M$  is set to  $N/3$  so that our centroid attention module compresses  $N$  input points into  $N/3$  centroids. The rest of the parts are kept unchanged. When decoding, the cross-attention is applied between the generated sequence and the centroids. We test two initialization schemes for the centroid attention, random sampling and mean pooling. Random sampling means we randomly sample  $N/3$  elements from the original sequence as the initial centroids, while mean pooling refers to apply mean pooling on every three elements.

Our baseline transformer follows the original encoder-decoder structure in Vaswani et al. (2017), with 4 layers in both encoder and decoder. We use a word embedding with 512 dimensions. All the models are trained for 30 epochs with Adam optimizer and the same learning rate. The number of warm-up steps is set to 4,000. At decode time, beam search with size 10 is exploited to generate the summary. Both self-attention and cross-attention is enabled in the decoder.

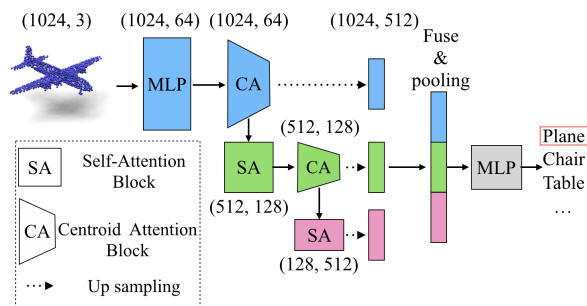


Figure 3: The architecture of the centroid transformer we used for point cloud classification. “CA” represents centroid attention and “SA” vanilla self-attention.

**Results** The results of the experiments is shown in Table. 1. Centroid transformer with mean-pooling initialization yields the highest score in all three metrics. Moreover,

our centroid transformer reduces 50% MACs against the original transformer on the encoder side. For the same Titan XP GPU, centroid transformer takes less storage space, allowing 38 more samples in a single batch. We also find the initialization scheme to be important. Random sampling scheme results in a centroid transformer that is worse than the baseline.

### 3.2 POINT CLOUD CLASSIFICATION

We apply our centroid transformer on point cloud classification. Point cloud data usually has over 1,000 points as input, which is a long sequence and hard to directly train with an original transformer. By applying our centroid transformer, we can gradually aggregate the thousands points into several abstract clusters, which brings powerful feature extraction ability and saves computational cost. We compare our method with several baselines including the state-of-the-art attention based method SepNet-W15 (Ran & Lu, 2020) on ModelNet40 dataset (Wu et al., 2015). We outperform the existing methods on classification accuracy and consume much less resource comparing with the attention based method SepNet-W15.

**Data** We use ModelNet40 as our benchmark, which has 40 classes with 9843 training shapes and 2468 test shapes. Consider that many of the ModelNet40 classification works use their specifically processed data, for a fair comparison, we use the same data as (Qi et al., 2017a), which is a uniformly sampled point cloud data from ModelNet40 raw data without any other specific normalization and preprocess.

**Model Configuration** We design a transformer architecture with 4 attention blocks and a 3-layer MLP classification head as Figure 3 shows. The first centroid attention block cluster  $N$  points to  $N/2$  and the second one abstract  $N/2$  to  $N/8$ . We use Farthest Point Sampling (FPS) as our initialization function. The dimension of the 4 attention locks is 64-128-128-512. We set  $K = 40$  in all the KNN masks and the KNN is calculated in feature space in the centroid attention blocks. After we extract features, we fuse the features in each layer by upsampling their number of points to  $N$  using nearest-neighbor sampling. Then we concatenate all the layers’ feature together and pass through a fully connected layer. The output feature will pass through a max pooling and a average pooling layer separately. At last, we concatenate them together as

the final feature of the input point cloud. The feature will pass a 3-layer MLP to get the final classification score. All the activation functions in the network are LeakyReLU with a negative slope of 0.2. We train the network with Adam optimizer start with  $1e^{-3}$  learning rate and decay by 0.7 every 20 epochs for 250 epochs in total.

Models	Acc	MACs(G)	Params(M)
PointNet (Qi et al., 2017a)	89.2	0.3	0.8
PointNet++ (Qi et al., 2017b)	91.9	7.9	12.1
DGCNN (Wang et al., 2019b)	92.8	2.4	2.0
SepNet-W15 (Ran & Lu, 2020)	93.1	22.4	4.8
Ours	<b>93.2</b>	5.4	4.1

Table 2: Results on ModelNet40 of our method and various of baselines. Here MACs denotes multiply-add cumulation and Params means the number of parameters in the model.

Method	Acc	Data/sec
Ours (T=1)	93.1	60
Ours (T=2)	93.2	55
Ours (T=3)	93.2	52
Random Sampling	91.7	312
Farthest Point Sampling	92.3	66
K-means	92.3	54

Table 3: Results on ModelNet40 of centroid attention when using different numbers of iterations  $T$  and different initialization strategies (see Eq (4)).

**Result** From Table 2, we can see that our model outperforms all the baseline on classification accuracy on ModelNet40. In addition, when comparing with SepNet-W15, our model can achieve a higher accuracy with only 1/4 MACs and fewer parameters.

**Ablation Study** In Table 3, we show the result of our method using different  $T$  in centroid attention blocks and compare them with other downsampling strategies. For the different  $T$ , the performance do not have a big difference. However, larger  $T$  means more computation operations, in practice, we choose  $T = 1$  for a performance-efficiency balance. For the downsampling strategies, we compare our model with Random Sampling, Farthest Point Sampling and K-means. We apply K-means for 3 iterations to guarantee the computation complexity is comparable with our centroid attention. Comparing with farthest point sampling strategy, our speed only slow a little bit while getting a 0.8 improvement in the classification accuracy. Comparing with the random sampling, we have a 1.5 accuracy improvement. In addition, we are 0.9 better than K-means.

**Visualization** We visualize our second centroid attention blocks’ feature cluster in Figure 4. We plot the sampled point in white star and its K-Nearest-Neighbour (KNNs) in red point. We set  $K = 40$  and use L2 distance in KNNs. From Figure 4 we can see that rather than gathering around the sampled point in the 3D space, the KNNs in our features space tend to distribute within the same se-

mantic part of the query part, which indicates our feature captures high-level concept of the shapes.

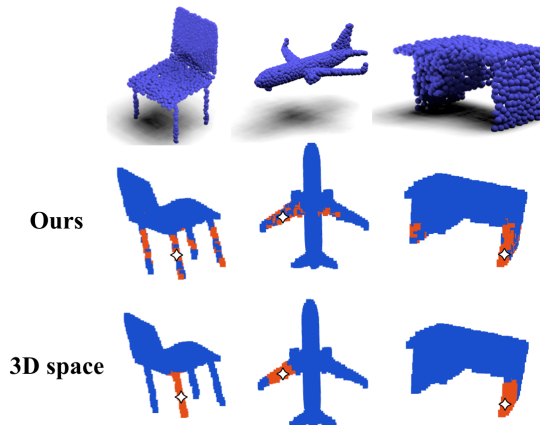


Figure 4: Learning classification on ModelNet40 with centroid transformer. We visualize the K-nearest-neighbours (KNNs) points of some sampled points (white stars). For the KNNs’ distance, for ours, we use the L2 distance in feature space learned in the second centroid attention blocks and for 3D space, we use the 3D euclidean distance. Here,  $K = 40$ , The red points indicates the KNNs points of the sampled white point.

### 3.3 POINT CLOUD RECONSTRUCTION

We further test our centroid attention block on point cloud reconstruction task and make a visualization plot to illustrate our layer’s efficiency and abstract ability. We use ShapeNet part and ShapeNet Core13 (Chang et al., 2015) as our dataset and use 3D Capsule Network (Zhao et al., 2019) as our backbone. We replace the Dynamic Routing module in the original capsule network with our centroid attention block to abstract the information from the prime capsules.

**Experiment Setup** We follow the 3D Capsule Network (Zhao et al., 2019) setting and construct an autoencoder to reconstruct the 3D point cloud with 2048 points. We set up two model scales with 12 and 64 latent capsules. In our centroid attention block, we treat the prime capsules as our input sequence and latent capsules as the abstract sequence. We use a linear projection to learn the initialization of the latent capsules. We set  $T = 3$  to match number of iterations in Dynamic Routing module.

For the 3D Capsule Network, we setup two network sizes, the small one contains 512 prime capsules with 16 dimensions and 12 latent capsules with 128 dimensions. The larger one contains 1024 prime capsules with 16 dimensions and 64 latent capsules with 64 dimensions. The 64 latent capsules setting keeps the same with the original setting in 3D capsule network. We train small setting for 200 epochs using ShapeNet Part dataset and base setting for 300 epochs using ShapeNet Core13 dataset. The other hyperparameter keeps the same as Zhao et al. (2019).

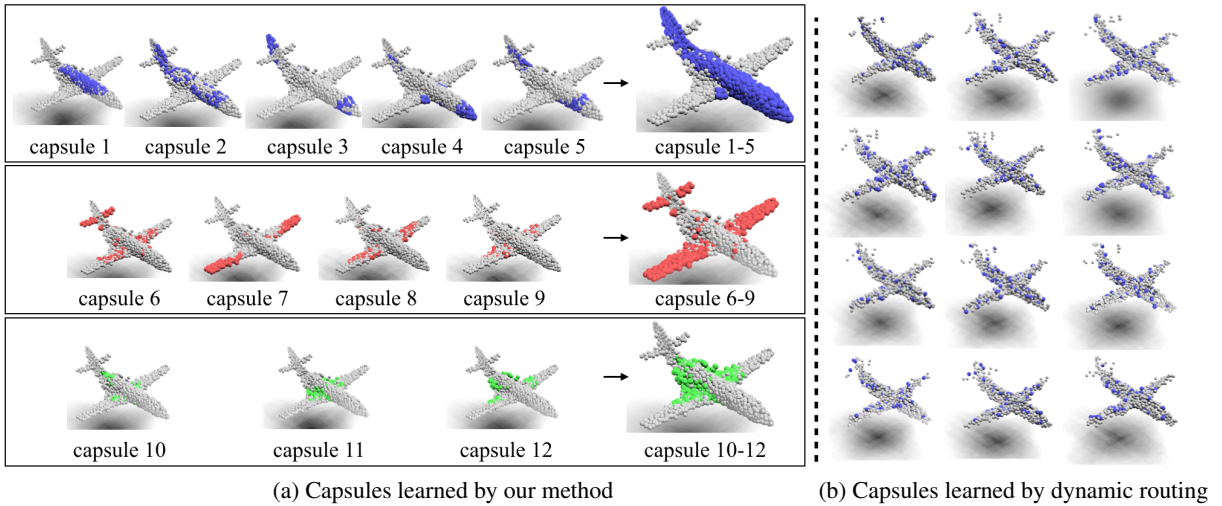


Figure 5: Point cloud reconstruction using 3D Capsule Network (Zhao et al., 2019) as backbone, with 12 latent capsules. We decode the 12 latent capsules one by one and highlight the corresponding decoded points with bright colors while keep the other parts gray. (a) shows the latent capsules learned by replacing the original dynamic routing module with centroid attention blocks, which can capture semantically meaningful parts of the plane, and are grouped into three clusters that represents plane body, plane front and back wings, and middle engine, respectively. (b) shows the capsules learned by dynamic routing in (Zhao et al., 2019), which distribute randomly and yield no semantic meanings.

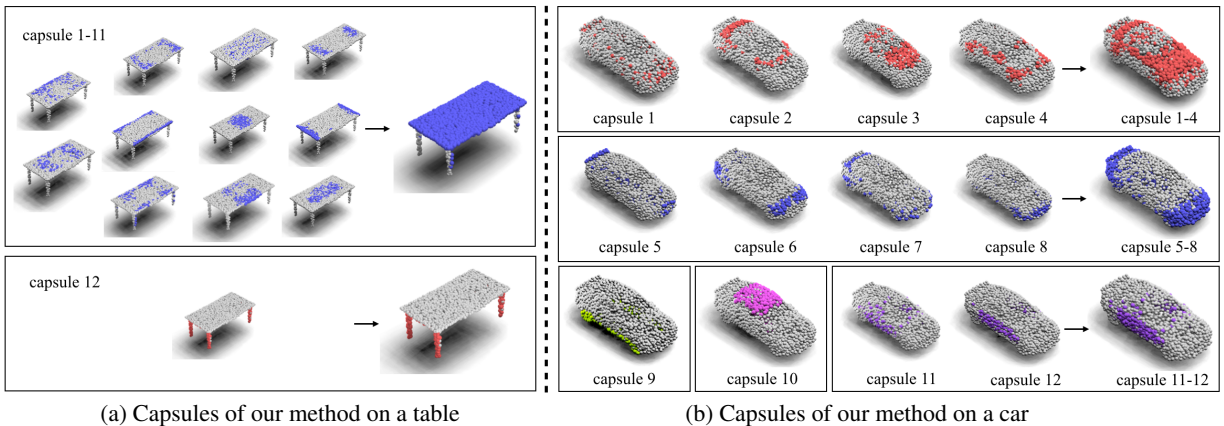


Figure 6: More visualization of capsules learned by our method. In both (a) and (b), the capsules map to semantically meaningful parties of the inputs.

**Result** From Table 4 we can see that in the 12 latent capsules setting, our model greatly outperforms the Dynamic Routing module to abstract the latent capsule and leads a Chamfer Distance  $1.6 \times 10^{-3}$  comparing with  $2.7 \times 10^{-3}$  in baseline. When comparing with Dynamic Routing in 64 latent capsules setting, which is same as the original paper, we still has  $10^{-3}$  better Chamfer Distance score comparing with baseline. The results indicate the Dynamic Routing module fails to abstract many prime capsules into a small amount of latent capsules. On the contrast, our centroid transformer can aggregate information no matter the output length is short or long.

Further, our centroid attention block has a much smaller parameter size as well as a larger max batch size per GPU.

Tjos means we can process more data in the same time and lead a much faster training speed comparing with the capsule network using Dynamic Routing. This roughly leads a  $3\times$  training speed boosting when training with same amount of GPUs.

**Visualization** We further visualize the decoded points from each latent capsule. To clearly show the semantic meaning, we use 12 latent capsules to plot the reconstruction visualization, in which each capsules can decode into 170 points. Each time, we highlight the decoded points from specific capsules in bright colors and keep the rest of the reconstruction points in gray. In Figure 5 (a), we show our learned latent capsules can capture semantic meanings and distribute on the specific part of the plane

# Cap	Method	CD( $\times 10^{-3}$ )	#Param(M)	MBS/GPU
12	DR	2.7	18.4	22
	Ours	<b>1.6</b>	<b>0.6</b>	<b>58</b>
64	DR	1.5	19.8	12
	Ours	<b>1.4</b>	<b>5.3</b>	<b>36</b>

Table 4: Comparison between the performance of dynamic routing and our centroid attention method under different latent capsules number settings (MBS/GPU = Maximum Batch Size per GPU, CD = Chamfer Distance). Here the Chamfer Distance is a metric for evaluating the quality of reconstruction.

shape. If we group several capsules together, we can further get the whole semantic parts. Figure 5 (b) shows the decoded points learned by Dynamic Routing. We can find that the reconstruction shape is in a low quality and the highlight points are in a random distribution across the whole shape. That means Dynamic Routing failed to learn a meaningful latent capsules under this setting. We plot two more visualization using our centroid attention blocks to show the result of different shapes with different number of semantic parts. Figure 6 (a) clearly shows that the table are decomposed into the surface and legs. Furthermore, Figure 6 (b) decomposes the car into body, surrounding, wheel, roof and door parts, these illustrate our centroid attention’s strong ability in clustering the semantic information.

### 3.4 VISION TRANSFORMER

We apply our centroid transformer structure on ImageNet (Deng et al., 2009) classification task using vision transformer to show our capacities among various transformer with large-scale data. We choose DeiT (Touvron et al., 2020) as our baseline, which is the state-of-the-art vision classification transformer structure on ImageNet dataset.

By applying centroid attention block in one specific layer, we build up our centroid transformer as Figure 7 shows. Our transformer abstract the image patches sequence into a shorter one in the middle, which reduces the computational cost comparing with the original DeiT. Further, we allow some overlaps in the first convolution layer to create a longer initial token sequence with richer represent ability.

We compare our centroid transformer with DeiT-tiny and DeiT-small, which are two vision transformers with different model scales. We also apply two efficient transformers, Set Transformer (Lee et al., 2019) and Linformer (Wang et al., 2020) on DeiT as baseline to compare the performance under an energy efficient setting.

**Experiment Setup** In the overlap setting, we set the first convolution layer with kernel size 16, stride 14, and padding 1. This can create a patch sequence with 256 tokens. In the centroid attention block, we first initialize our shorter sequence by reshaping the  $N$  length patch tokens into a  $\sqrt{N} \times \sqrt{N}$  order. We then apply a depth-wise

Models	#layers	#tokens	embedding dimension	centroid @
DeiT-tiny		196		-
Ours-1	12	196	192	6
Ours-2		256		5
Ours-3		256		7
DeiT-small		196		-
Ours-4	12	196	384	6
Ours-5		256		5
Ours-6		256		7

Table 5: Architecture design of different models for image classification tasks on ImageNet, centroid @ means replacing the self-attention block with the centroid attention block at specific layer.

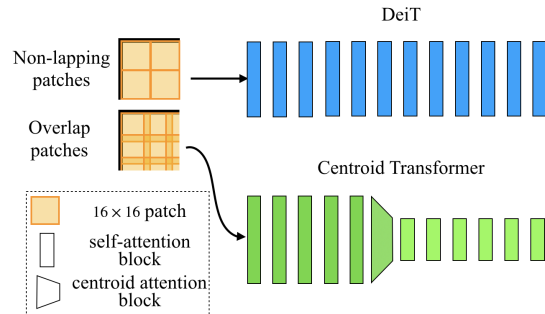


Figure 7: Comparing DeiT and centroid transformer for image inputs. Upper panel: DeiT partitions the input image into non-lapping patches and keeps the same number of patches throughout the layers, which may lose information of the image because the patches do not overlap. In comparison, thanks to the ability of down-sampling, the centroid transformer with comparable computational cost can take a larger number of overlapping patches in the early stage and hence capture more information from the input images.

convolution layer with kernel size 3, stride 2, padding 1 to downsample the input tokens into  $\sqrt{N}/2 \times \sqrt{N}/2$  and reshape it back to  $N/4$  tokens as the initialization. We set  $T = 1$  for a better performance-efficiency trade off. The rest of the training setting are the same as DeiT. We setup different model scales. The overall architectures design is listed in Table 5. For fast transformer baselines, we set Linformer’s project dimension  $k = 128$  and Set Transformer’s induce point set length  $m = 128$ .

**Result** Our results are shown in Tabel 6. In “Ours-1” and “Ours-4” setting, by replacing one self-attention blocks into centroid attention block, our model has only 64% MACs comparing the original DeiT-tiny and DeiT-small while only drop the Top-1 Accuracy by 0.4 and 0.3. Further, when we allow a longer initial sequence by overlapping the image patches and adjust the centroid attention blocks to the fifth layer, the centorid block “Ours-2” and “Ours-5” achieves a same and 0.2 higher top-1 with 81% MACs. When we further increase the MACs by adjusting the centroid attention block’s layer, we can get larger

models “Ours-3” and “Ours-6” with the close MACs comparing with DeiT-tiny and DeiT-small baseline and gains 1.2 and 1.0 performance improvement.

Whatsmore, when we compare centroid transformer with other fast transformers, we outperform set transformer by over 5.0 and linformer by over 2.0 Top-1 accuracy with smaller MACs. Our good performance comparing with these fast transformers further shows our structures’ powerful ability and efficiency to handle even this kind of large-scale image classification task.

Method	Top-1 Acc	MACs(G)	Params(M)
Set Transformer	66.1	1.1	5.9
Linformer	69.9	1.2	6.3
DeiT-tiny	72.2	1.3	5.7
Ours-1	71.8	0.8	5.7
Ours-2	72.2	1.0	5.7
Ours-3	<b>73.4</b>	1.3	5.8
Set Transformer	74.6	3.8	22.4
Linformer	77.6	4.4	22.6
DeiT-small	79.9	4.7	22.1
Ours-4	79.6	2.9	22.1
Ours-5	80.1	3.6	22.1
Ours-6	<b>80.9</b>	4.7	22.3

Table 6: Vision Transformer result compared with DeiT. Ours-x indicates different MACs setting of our model. MACs indicates multiply-add cumulation and Params means the number of parameters in the model.

## 4 RELATED WORKS

**Fast Transformers** A line of recent works have been developed to approximate self-attention layers to improve over the  $O(N^2)$  complexity. These methods keep the basic design of self-attention, mapping  $N$  inputs to  $N$  outputs, and is hence different in purpose with our method, which compresses  $N$  inputs to a smaller number  $M$  of outputs. Among these works, Reformer (Kitaev et al., 2019) uses Locally Sensitive Hashing to accelerate attention, yielding a  $O(N \log N)$  complexity; LongFormer (Beltagy et al., 2020) works by combining sparse global attention with local attention; Linear Transformers (Katharopoulos et al., 2020)/ Linformer (Wang et al., 2020)/ Efficient Attention (Shen et al., 2018) achieve linear  $O(N)$  complexity by low-rank approximation. Set Transformer (Lee et al., 2019) reduces the computation by introducing a set of induced points, which plays a role similar to centroids, only serve as the intermediary layer between  $N$  inputs and  $N$  outputs. Another related work is Routing Transformers (Roy et al., 2020), which introduces a sparse routing module based on online k-means, reducing the complexity of attention to  $O(n^{1.5})$ .

PoWER-BERT (Goyal et al., 2020) also reduces the number of tokens gradually to improve the efficiency of BERT. However, their work fundamentally differs from ours from three aspects: (1) Their work is motivated by the phenomenon of information diffusion in BERT specifically,

which may not be the case in other transformers. (2) Their work focus on *select* a subset of tokens from the original sequence, while the emphasis of our work is *summarize* the information into several centroids. This leads to completely distinct structure design. (3) Their scoring function is human-designed. In contrast, we start from clustering algorithm, and derives a novel connection between gradient-based clustering and attention.

**Capsule Networks** Similar to our method, capsule networks (Hinton et al., 2011) are also based on the idea of “building clustering algorithms into neural networks”. Different from our method, which is based on amortizing gradient-based clustering algorithms, Dynamic routing and EM routing (Sabour et al., 2017; Wang & Liu, 2018; Hinton et al., 2018) in capsule networks are based on amortizing EM like algorithms. However, unlike our method, dynamic routing and EM routing are not trainable modules and hence not as efficient as our method in extracting data information. In addition, our method does not need to store the pairwise assignment information like dynamic/EM routing and hence reduces the runtime space consumption.

**Adaptive Down-sampling** At a high level, our method can be viewed as an attention-like mechanism for adaptively down-sampling the inputs, which forms a key building block for deep neural networks in computer vision. In convolutional neural networks, various techniques have been proposed, including fixed strategies such as pooling (Simonyan & Zisserman, 2014), strided convolution (Springenberg et al., 2014), dilated convolution (Yu & Koltun, 2015), learnable down-sampling techniques such as Local-importance based pooling (Gao et al., 2019), deformable convolution (Dai et al., 2017), and trainable Region-of-Interest (ROI) Pooling (Gu et al., 2018). In addition, Nezhadarya et al. (2020) proposes an adaptive down-sampling layer for point cloud classification. RandLA-Net (Hu et al., 2020) uses random-sampling to process large-scale point cloud. Comparing these methods, which mostly focus on convolutional neural networks (CNNs), our method provides a general and basic adaptive down-sampling strategy for transformers, which is expected to find important applications as the counterparts in CNNs.

**Metric Learning for Clustering** A line works have been developed to learn domain-specific similarity functions to boost the performance of the clustering algorithms based on the learned metrics (Yang et al., 2016, 2017; Hsu et al., 2018; Aljalbout et al., 2018; Yang et al., 2019). This yields a metric learning task. Our work is fundamentally different we use clustering to inspire the design of a new transformer architecture, and our goal is not to actually optimize the clustering quality for a specific problem.



## 5 CONCLUSION

In this paper, we propose centroid attention, which performs summative reasoning for sequence modeling. Centroid attention takes the original sequence as input, and provides a shorter sequence of centroids that absorbs the information of the input sequence. We use centroid attention to construct centroid transformer. By using centroids for later stages, the computational and memory consumption of centroid transformers is significantly reduced against their full-length counterparts. Experiments conducted on text summarization, 3D vision and image processing demonstrates centroid transformers can yield similar / better performance over the original transformers with high efficiency.

## REFERENCES

- Aljalbout, E., Golkov, V., Siddiqui, Y., Strobel, M., and Cremers, D. Clustering with deep learning: Taxonomy and new methods. *arXiv preprint arXiv:1801.07648*, 2018.
- Beltagy, I., Peters, M. E., and Cohan, A. Longformer: The long-document transformer. *arXiv preprint arXiv:2004.05150*, 2020.
- Carion, N., Massa, F., Synnaeve, G., Usunier, N., Kirillov, A., and Zagoruyko, S. End-to-end object detection with transformers. In *European Conference on Computer Vision*, pp. 213–229. Springer, 2020.
- Chang, A. X., Funkhouser, T., Guibas, L., Hanrahan, P., Huang, Q., Li, Z., Savarese, S., Savva, M., Song, S., Su, H., et al. Shapenet: An information-rich 3d model repository. *arXiv preprint arXiv:1512.03012*, 2015.
- Dai, J., Qi, H., Xiong, Y., Li, Y., Zhang, G., Hu, H., and Wei, Y. Deformable convolutional networks. In *Proceedings of the IEEE international conference on computer vision*, pp. 764–773, 2017.
- Deng, J., Dong, W., Socher, R., Li, L.-J., Li, K., and Fei-Fei, L. Imagenet: A large-scale hierarchical image database. In *2009 IEEE conference on computer vision and pattern recognition*, pp. 248–255. Ieee, 2009.
- Dosovitskiy, A., Beyer, L., Kolesnikov, A., Weissenborn, D., Zhai, X., Unterthiner, T., Dehghani, M., Minderer, M., Heigold, G., Gelly, S., et al. An image is worth 16x16 words: Transformers for image recognition at scale. *arXiv preprint arXiv:2010.11929*, 2020.
- Gao, Z., Wang, L., and Wu, G. Lip: Local importance-based pooling. In *Proceedings of the IEEE International Conference on Computer Vision*, pp. 3355–3364, 2019.
- Goyal, S., Choudhury, A. R., Raje, S., Chakaravarthy, V., Sabharwal, Y., and Verma, A. Power-bert: Accelerating bert inference via progressive word-vector elimination. In *International Conference on Machine Learning*, pp. 3690–3699. PMLR, 2020.
- Gu, J., Hu, H., Wang, L., Wei, Y., and Dai, J. Learning region features for object detection. In *Proceedings of the European Conference on Computer Vision (ECCV)*, pp. 381–395, 2018.
- Hinton, G. E., Krizhevsky, A., and Wang, S. D. Transforming auto-encoders. In *International conference on artificial neural networks*, pp. 44–51. Springer, 2011.
- Hinton, G. E., Sabour, S., and Frosst, N. Matrix capsules with em routing. In *International conference on learning representations*, 2018.
- Hsu, Y.-C., Lv, Z., and Kira, Z. Learning to cluster in order to transfer across domains and tasks. In *International Conference on Learning Representations (ICLR)*, 2018.
- Hu, Q., Yang, B., Xie, L., Rosa, S., Guo, Y., Wang, Z., Trigioli, N., and Markham, A. Randa-net: Efficient semantic segmentation of large-scale point clouds. In *Proceedings of the IEEE/CVF Conference on Computer Vision and Pattern Recognition*, pp. 11108–11117, 2020.
- Irie, K., Zeyer, A., Schlüter, R., and Ney, H. Language modeling with deep transformers. *arXiv preprint arXiv:1905.04226*, 2019.
- Jiao, X., Yin, Y., Shang, L., Jiang, X., Chen, X., Li, L., Wang, F., and Liu, Q. Tinybert: Distilling bert for natural language understanding. In *Proceedings of the 2020 Conference on Empirical Methods in Natural Language Processing: Findings*, pp. 4163–4174, 2020.
- Katharopoulos, A., Vyas, A., Pappas, N., and Fleuret, F. Transformers are rnns: Fast autoregressive transformers with linear attention. In *International Conference on Machine Learning*, pp. 5156–5165. PMLR, 2020.
- Kitaev, N., Kaiser, L., and Levskaya, A. Reformer: The efficient transformer. In *International Conference on Learning Representations*, 2019.
- Lee, J., Lee, Y., Kim, J., Kosiorek, A., Choi, S., and Teh, Y. W. Set transformer: A framework for attention-based permutation-invariant neural networks. In *International Conference on Machine Learning*, pp. 3744–3753. PMLR, 2019.
- Lin, C.-Y. Rouge: A package for automatic evaluation of summaries. In *Text summarization branches out*, pp. 74–81, 2004.
- Nallapati, R., Zhou, B., Gulcehre, C., Xiang, B., et al. Abstractive text summarization using sequence-to-sequence rnns and beyond. *arXiv preprint arXiv:1602.06023*, 2016.
- Nezhadarya, E., Taghavi, E., Razani, R., Liu, B., and Luo, J. Adaptive hierarchical down-sampling for point cloud classification. In *Proceedings of the IEEE/CVF Conference on Computer Vision and Pattern Recognition*, pp. 12956–12964, 2020.
- Qi, C. R., Su, H., Mo, K., and Guibas, L. J. Pointnet: Deep learning on point sets for 3d classification and segmentation. In *Proceedings of the IEEE conference*

- on computer vision and pattern recognition, pp. 652–660, 2017a.
- Qi, C. R., Yi, L., Su, H., and Guibas, L. J. Pointnet++: Deep hierarchical feature learning on point sets in a metric space. *arXiv preprint arXiv:1706.02413*, 2017b.
- Ramsauer, H., Schäfl, B., Lehner, J., Seidl, P., Widrich, M., Gruber, L., Holzleitner, M., Pavlović, M., Sandve, G. K., Greiff, V., et al. Hopfield networks is all you need. *arXiv preprint arXiv:2008.02217*, 2020.
- Ran, H. and Lu, L. Deeper or wider networks of point clouds with self-attention? *arXiv preprint arXiv:2011.14285*, 2020.
- Roy, A., Saffar, M., Vaswani, A., and Grangier, D. Efficient content-based sparse attention with routing transformers. *arXiv preprint arXiv:2003.05997*, 2020.
- Rush, A. M., Chopra, S., and Weston, J. A neural attention model for abstractive sentence summarization. *arXiv preprint arXiv:1509.00685*, 2015.
- Sabour, S., Frosst, N., and Hinton, G. E. Dynamic routing between capsules. *arXiv preprint arXiv:1710.09829*, 2017.
- Shen, Z., Zhang, M., Zhao, H., Yi, S., and Li, H. Efficient attention: Attention with linear complexities. *arXiv preprint arXiv:1812.01243*, 2018.
- Simonyan, K. and Zisserman, A. Very deep convolutional networks for large-scale image recognition. *arXiv preprint arXiv:1409.1556*, 2014.
- Springenberg, J. T., Dosovitskiy, A., Brox, T., and Riedmiller, M. Striving for simplicity: The all convolutional net. *arXiv preprint arXiv:1412.6806*, 2014.
- Touvron, H., Cord, M., Douze, M., Massa, F., Sablayrolles, A., and Jégou, H. Training data-efficient image transformers and distillation through attention. *arXiv preprint arXiv:2012.12877*, 2020.
- Vaswani, A., Shazeer, N., Parmar, N., Uszkoreit, J., Jones, L., Gomez, A. N., Kaiser, L., and Polosukhin, I. Attention is all you need. In *Advances in neural information processing systems*, pp. 5998–6008, 2017.
- Wang, D. and Liu, Q. An optimization view on dynamic routing between capsules. 2018.
- Wang, Q., Li, B., Xiao, T., Zhu, J., Li, C., Wong, D. F., and Chao, L. S. Learning deep transformer models for machine translation. *arXiv preprint arXiv:1906.01787*, 2019a.
- Wang, S., Li, B., Khabsa, M., Fang, H., and Ma, H. Linformer: Self-attention with linear complexity. *arXiv preprint arXiv:2006.04768*, 2020.
- Wang, Y., Sun, Y., Liu, Z., Sarma, S. E., Bronstein, M. M., and Solomon, J. M. Dynamic graph cnn for learning on point clouds. *Acm Transactions On Graphics (tog)*, 38(5):1–12, 2019b.
- Wu, Z., Song, S., Khosla, A., Yu, F., Zhang, L., Tang, X., and Xiao, J. 3d shapenets: A deep representation for volumetric shapes. In *Proceedings of the IEEE conference on computer vision and pattern recognition*, pp. 1912–1920, 2015.
- Yang, B., Fu, X., Sidiropoulos, N. D., and Hong, M. Towards k-means-friendly spaces: Simultaneous deep learning and clustering. In *international conference on machine learning*, pp. 3861–3870. PMLR, 2017.
- Yang, J., Parikh, D., and Batra, D. Joint unsupervised learning of deep representations and image clusters. In *Proceedings of the IEEE conference on computer vision and pattern recognition*, pp. 5147–5156, 2016.
- Yang, L., Zhan, X., Chen, D., Yan, J., Loy, C. C., and Lin, D. Learning to cluster faces on an affinity graph. In *Proceedings of the IEEE Conference on Computer Vision and Pattern Recognition (CVPR)*, 2019.
- Yu, F. and Koltun, V. Multi-scale context aggregation by dilated convolutions. *arXiv preprint arXiv:1511.07122*, 2015.
- Zhang, J., Luan, H., Sun, M., Zhai, F., Xu, J., Zhang, M., and Liu, Y. Improving the transformer translation model with document-level context. *arXiv preprint arXiv:1810.03581*, 2018.
- Zhao, Y., Birdal, T., Deng, H., and Tombari, F. 3d point capsule networks. In *Proceedings of the IEEE/CVF Conference on Computer Vision and Pattern Recognition*, pp. 1009–1018, 2019.

## A AN ENERGY VIEW OF SELF-ATTENTION

We provide another view to draw connection between attention mechanism and learning to abstract with energy-based models. Let's first rewrite the self-attention operation in an energy-view. We start by defining the following energy function on the sequence  $\{\mathbf{x}_i\}_{i=1}^N$ ,

$$E(\{\mathbf{x}_i\}_{i=1}^N) = \sum_{i=1}^N \sum_{j=1}^N \zeta(\mathbf{x}_i^\top \mathbf{x}_j), \quad (5)$$

where  $\zeta(\cdot, \cdot)$  is a pairwise energy function. To find the sequence with the lowest energy, we can perform gradient descent yielding,

$$\mathbf{x}_i \leftarrow \mathbf{x}_i - \epsilon \sum_{j=1}^N \nabla_{\mathbf{x}_i} \zeta(\mathbf{x}_i^\top \mathbf{x}_j) \mathbf{x}_j, \quad \forall i = 1, \dots, N. \quad (6)$$

Properly setting  $\zeta(\mathbf{x}_i^\top \mathbf{x}_j)$  will recover the single-headed self-attention operation with  $v(x_j) = x_j$  and a similarity function without the normalization denominator in Eq. (2). In this sense, self-attention can be explained as one gradient step towards the sequence with the lowest energy.

The energy function above yields a fully observed pairwise energy function. The centroid attention can be viewed as corresponding to the energy function of restricted Boltzmann machine (RBM) in which  $\{\mathbf{u}_j\}_{j=1}^M$  are viewed as hidden variables,

$$E(\{\mathbf{x}_i\}_{i=1}^N, \{\mathbf{u}_j\}_{j=1}^M) = \sum_{i=1}^N \sum_{j=1}^M \zeta(\mathbf{u}_j^\top \mathbf{x}_i). \quad (7)$$

Here,  $\{\mathbf{x}_i\}_{i=1}^N$  are the visible variables, and  $\{\mathbf{u}_j\}_{j=1}^M$  are the hidden variables. Given fixed visible variables, we can also find the hidden variables that minimizes the energy by gradient descent,

$$\mathbf{u}_j \leftarrow \mathbf{u}_j - \epsilon \sum_{i=1}^N \nabla_{\mathbf{u}_j} \zeta(\mathbf{x}_i^\top \mathbf{u}_j) \mathbf{x}_i, \quad \forall j = 1, \dots, M. \quad (8)$$

Therefore, centroid attention is like finding the most likely hidden variable for a given observed variable. Note that the derivation here is different from the one in the main text, because the similarity function is not normalized here.